Characterization of Ferrous FixL−Nitric Oxide Adducts by Resonance Raman Spectroscopy†

Gudrun S. Lukat-Rodgers and Kenton R. Rodgers*

Department of Chemistry, North Dakota State University, Fargo, North Dakota 58105

Received November 14, 1996; Revised Manuscript Received February 3, 1997⊗

ABSTRACT: Resonance Raman spectra of the nitric oxide adducts of the ferrous forms of two soluble truncations of *Rhizobium meliloti* FixL, FixL* and FixLN, are reported. At room temperature, four isotope sensitive vibrations are observed for both ferrous FixL*−NO and ferrous FixLN−NO. For FixL*−NO, they are observed at 558, 525, 450, and 1675 cm^{-1} and are assigned to ν(Fe−NO) of a six-coordinate nitrosyl adduct, ν(Fe−NO) of a five-coordinate nitrosyl adduct, δ(Fe−NO) of a six-coordinate nitrosyl adduct, and ν(N−O) of a five-coordinate nitrosyl adduct, respectively. Similar frequencies are observed for the FixLN−NO isotope sensitive bands. On the basis of the frequencies and spectral separation of the ν(Fe−NO) and δ(Fe−NO) modes, the Fe−N−O unit is concluded to have a bent geometry similar to those observed for the nitrosyl adducts of ferrous hemoglobin and myoglobin. Both proteins can be converted to predominantly five-coordinate nitrosyl adducts by lowering the temperature. In low-temperature resonance Raman spectra of FixL*−NO and FixLN−NO, the 558 cm^{-1} bands are significantly decreased in intensity and $\nu(Fe-NO)_{5-c}$ (the Fe−NO stretching vibration for the five-coordinate nitrosyl adduct) is observed at 529 and 526 cm^{-1}, respectively. Analysis of the ν_3 and ν_8 vibrations for these nitrosyl adducts also supports the presence of both five- and six-coordinate nitrosyl adducts of FixL* and FixLN at room temperature and the conversion to predominantly five-coordinate nitrosyl adducts at low temperatures. This temperature-dependent interconversion is reversible. The possible physiological relevance of the thermally accessible five-coordinate state is discussed. The width of $\nu(Fe-NO)_{6-c}$ at half-height is 1.3 times broader in FixLN−NO than in FixL*−NO, suggesting that the Fe−N−O geometry is more homogeneous in FixL*−NO. In low-temperature spectra of FixLN−NO, a second $\nu(N-O)_{5-c}$ band is observed, indicating that more than one conformation is attainable in the five-coordinate FixLN−NO. This second $\nu(N-O)_{5-c}$ is not observed for five-coordinate FixL*−NO, further suggesting a more conformationally restricted nitrosyl heme in FixL*. These variations in the vibrations involving the Fe−NO unit indicate that the kinase domain influences the heme structure. The spectral differences are discussed in terms of the interdomain interactions that result in ligation-dependent mediation of the kinase activity.

The soil bacterium *Rhizobium meliloti* establishes a symbiotic association with alfalfa, which facilitates nitrogen fixation. Here the cells respond to reduced oxygen tension by expression of genes needed for nitrogen fixation (*nif* and *fix* genes). The initial step in signal transduction responsible for expression of the regulatory genes *nifA* and *fixK* occurs at the sensor protein, FixL (David et al., 1988). *R. meliloti* FixL is a membrane-bound protein which has a heme-containing domain and a kinase domain (Gilles-Gonzalez et al., 1991; Monson et al., 1992). When O_2 is bound to the heme iron, FixL kinase activity is inhibited. At low oxygen concentrations, oxyFixL releases O_2, leaving the heme in its deoxy form. In deoxyFixL, autophosphorylation activity is enhanced, and FixL−phosphate is produced in order to provide phosphoryl groups to the response regulator, FixJ (Lois et al., 1993). FixJ−phosphate is a transcriptional activator for *nifA* and *fixK* (Reyrat et al., 1993; Galinier et al., 1994). Hence, the cellular response to low oxygen tension is initiated by the generation of deoxyFixL.

The mechanism for regulation of the kinase activity of FixL is dependent on the spin state of the heme iron (Gilles-Gonzalez et al., 1995). Kinase activity is maximized when the iron is high-spin, *i.e.* deoxyFixL. When O_2 binds to the heme, the heme iron is converted to the low-spin state, and the kinase domain is inactivated. This spin state change can be triggered by other heme ligands like CN^-, CO, and NO. *Rhizobium* bacteria generate NO as an intermediate in their denitrification process (Chan & Weatcroft, 1993). Hence, it has been suggested that under certain conditions FixL may also serve as a NO receptor (Gilles-Gonzalez et al., 1994).

An understanding of the structural and electronic features of the ferrous nitrosyl adduct of FixL is important from two perspectives. First, nitric oxide binds to ferrous heme proteins (Deatherage & Maffat, 1979; Scheidt et al., 1977; Scheidt & Piciulo, 1976; Schiedt & Frisse, 1975; Piciulo et al., 1974) to yield adducts that are similar in electronic structure and geometry to the physiologically important dioxygen adducts (Shaanan, 1982; Philips, 1980; Jameson et al., 1978, 1980; Collman et al., 1974). Thus, it is expected that ferrous FixL−NO will be a good model for the deactivated form of FixL, oxyFixL. Second, in light of

† This research was supported by USDA Grant 96-35305-3628, the North Dakota State University (NDSU) Chemistry Department, the NDSU Graduate College, the NDSU College of Science and Math, the North Dakota EPSCoR, and the United States Department of Agriculture. K.R.R. is the recipient of a Presidential Early Career Award.

* Author to whom correspondence should be addressed.

⊗ Abstract published in *Advance ACS Abstracts,* March 15, 1997.

S0006-2960(96)02823-1 CCC: $14.00

FixL's potential role as a NO sensor, characterization of the ferrous nitrosyl adduct will be useful in elucidation of potential mechanism(s) for NO sensing.

In the resonance Raman study reported here, two deletion derivatives of *R. meliloti* FixL, FixLN (heme domain only) and FixL*(functional heme kinase) (Monson et al., 1992), were investigated. The resonance Raman data reveal that ferrous FixLN−NO exists as both five- and six-coordinate (hereafter indicated by 5-c and 6-c, respectively) nitrosyl adducts at room temperature. The presence of the kinase domain in ferrous FixL*−NO influences both the position of this equilibrium and the conformational homogeneity of the nitrosyl heme.

MATERIALS AND METHODS

A soluble truncated FixL (FixL*) and the heme-containing domain of FixL (FixLN) of *R. meliloti* were expressed from TG1(pGG820) and TG1(pEM130), respectively (Monson et al., 1992). Both proteins were purified as previously described (Monson et al., 1992). Protein purity was assayed via SDS−PAGE and examination of the visible spectrum in the Soret region of the spectrum. Autophosphorylation activity of purified FixL* was confirmed by anaerobic phosphorylation assays previously described (Gilles-Gonzalez et al., 1991; Rodgers et al., 1996).

The deoxy form of both FixL* and FixLN were generated under anaerobic conditions by the addition of excess of sodium dithionite. Complete reduction was determined by monitoring the visible spectrum of the samples. The heme−$^{14}N^{16}O$ derivatives were prepared by equilibration of the deoxyFixLs with 1 atm of $^{14}N^{16}O$ (99.0%). For the isotope experiments, FixL−$^{15}N^{18}O$ adducts were prepared with $^{15}N^{18}O$ (99.4%).

Resonance Raman spectra were obtained at 20 and −45 °C for 70 μM protein samples prepared in 80 mM sodium phosphate (pH 7.8) and 5% glycerol. The spectra were acquired from samples in a spinning 5 mm NMR tube using the 135° backscattering geometry and f_1 collection. Either the 406.7 nm or the 413.1 nm line from a Kr ion laser was used for Raman excitation, and 20 mW of laser power was focused to a line (3 mm) using a cylindrical lens to minimize photolysis artifacts and laser-induced sample degradation. This laser power was chosen, as it did not result in measurable NO photolysis in the frozen solutions, as judged by lack of observable ν_4 (most intense peak in the spectrum) for the deoxy heme. Scattered light was passed through a holographic notch filter and a polarization scrambler then *f*-matched to a 0.67 m single spectrograph fitted with a 110 × 110 mm grating having a groove density of 2400 grooves/mm. The Raman spectrum was detected using a 25 mm LN_2-cooled CCD camera under the control of a microcomputer. Spectra were calibrated against toluene and DMF. The sample tube was spun at *ca.* 20 Hz to minimize NO photolysis and to avoid laser-induced damage to the protein. Absorption spectra were obtained before and after the resonance Raman experiments to verify that the protein had not been degraded by exposure to the laser beam. Resonance Raman spectra of deoxyFixLN and deoxyFixL* were obtained under conditions identical to those used for the FixL−NO adducts in order to identify any features due to photoproduct in the Raman spectra.

Sample temperatures were achieved using a variable-temperature system constructed in our laboratory. This system has the sample tube suspended in a liquid N_2 boil-off stream. The temperature of the sample is monitored by a thermocouple placed as close as possible to the sample tube without touching it. The temperature is controlled to ±1 °C with a heater placed before the sample in the boil-off stream.

RESULTS

Anaerobic reduction of FixLN (or FixL*) with sodium dithionite followed by addition of nitric oxide generates a FixLN (FixL*) nitrosyl adduct, with the visible spectrum shown in the inset of Figure 1a. Parts a and b of Figure 1 contain the low- and high-frequency regions of the room-temperature resonance Raman spectra of the FixLN and FixL* nitrosyl adducts obtained with 406.7 nm excitation. In the low-frequency regions of these spectra, the 676 (675) and 754 (753) cm^{-1} bands are assigned to the ν_7 and ν_{15} modes (Abe et al., 1978; Kitagawa et al., 1978), respectively. In the high-frequency region, the most prominent feature, ν_4, is observed at 1373 (1374) cm^{-1}. This is similar to ν_4 frequencies observed for other heme protein nitrosyl adducts (Benko & Yu, 1983; Hu & Kincaid, 1991; Deinum et al., 1996). The frequency of ν_3, one of the porphyrin core size marker bands, increases as the porphyrin core size (the distance between the porphyrin ring center and the pyrrole nitrogen atom) approaches its natural size (Spaulding et al., 1975; Parthasarathi et al., 1987). The core sizes of FixLN−NO (ν_3 at 1498 cm^{-1}) and FixL*−NO (ν_3 at 1498 cm^{-1}) are similar at 1.99 Å, and comparable to that reported for ferrous nitrosyl myoglobin, 1.98 Å (Benko & Yu, 1983; Hu & Kincaid, 1991). These core sizes are calculated using empirical linear relationships that correlate crystallographic core sizes with the core size marker band frequencies (Parthasarathi et al., 1987). The ν_{10}, $\nu_{C=C}$, and ν_2 bands in the high-frequency spectrum are assigned for FixLN−NO and FixL*−NO on the basis of their polarizations and by analogy to ferrous nitrosyl hemoglobin and guanylate cyclase (Nagai et al., 1980; Deinum et al., 1996). The parallel and perpendicular resonance Raman spectra of FixLN−NO in Figure 1c reveal the depolarized heme vibrations.

The low- and high-frequency regions of the resonance Raman spectrum of deoxyFixLN obtained with 406.7 nm excitation are shown in Figure 2. These data are included to verify that the FixLN−NO adducts were not contaminated with deoxyFixLN. The low-frequency region of the deoxy-FixLN resonance Raman spectrum has several intense bands which are assigned by analogy to their counterparts in deoxymyoglobin and cyctochrome *c* peroxidase (Rousseau & Friedman, 1988; Smulevich et al., 1996). They are ν_6 (792 cm^{-1}), ν_7 (675 cm^{-1}), and ν_{15} (757 cm^{-1}). The ν_6, ν_7, and ν(Fe−His) (212 cm^{-1}) (Rodgers et al., 1996) bands in deoxyFixLN are intense with 406.7 and 413.1 nm excitation; the ν_6 and ν(Fe−His) for deoxyFixLN are readily apparent when ferrous FixLN−NO samples are contaminated with deoxyFixLN due to photodissociation of NO. Similar low-frequency resonance Raman results were obtained for deoxy-FixL* (data not shown) (Rodgers et al., 1996). Assignment of the deoxy bands in the high-frequency region can be made by analogy to those observed for other ferrous heme proteins; 1354, 1470, 1557, 1602, and 1620 cm^{-1} bands are assigned to ν_4, ν_3, ν_2, ν_{10}, and $\nu_{C=C}$, respectively (Choi et al., 1982; Rousseau & Friedman, 1988; Deinum et al., 1996). The

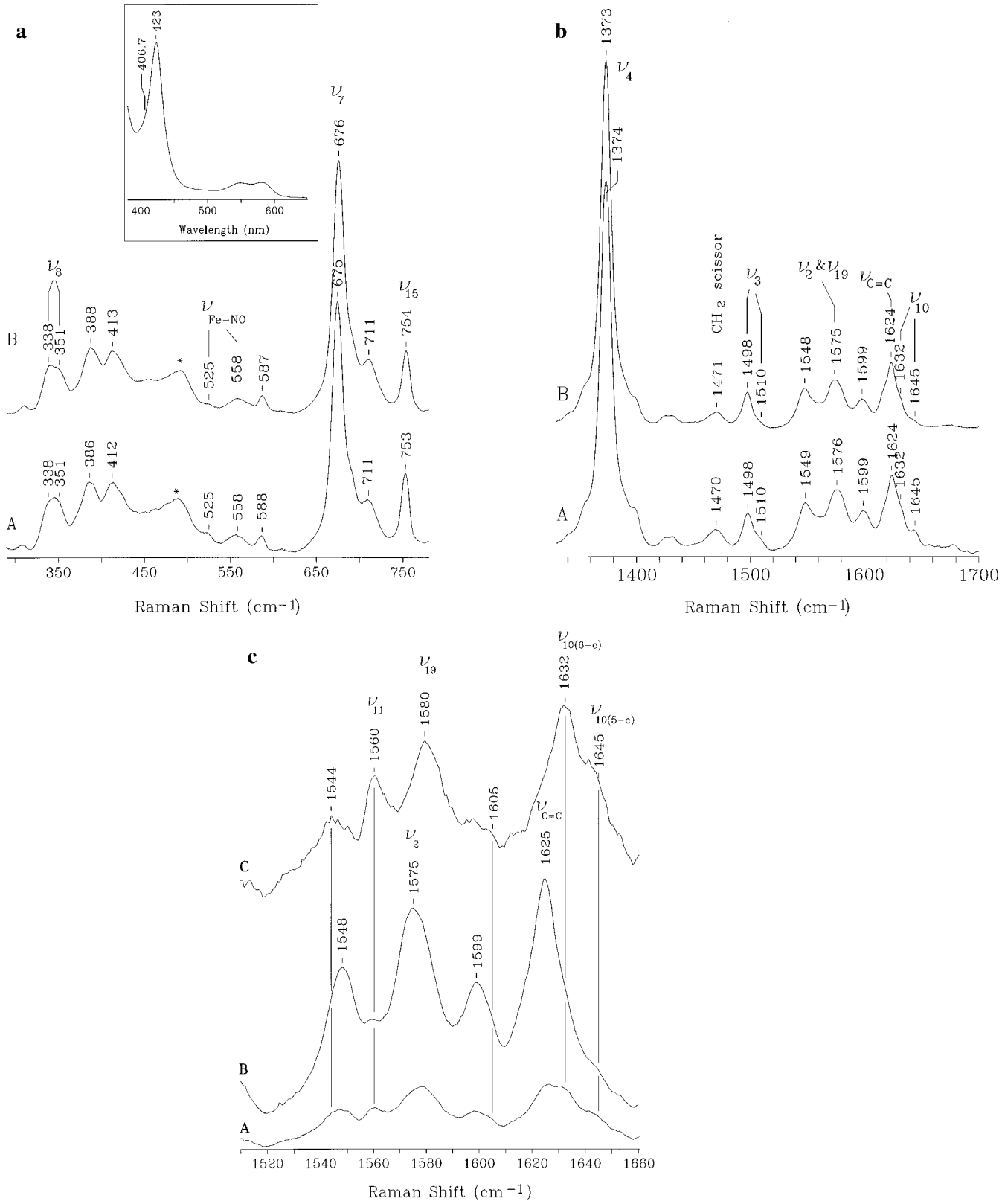

FIGURE 1: (a) Low-frequency resonance Raman spectra of (A) ferrous FixL*−NO and (B) ferrous FixLN−NO at 20 °C with 406.7 nm laser excitation. The protein concentration was 70 μM in 80 mM sodium phosphate buffer (pH 7.8) and 5% glycerol. Assignments of the in-plane heme vibrations were made by analogy with Mb−NO and Hb−NO. The asterisk indicates an underlying glass band. (inset) The electronic absorption spectrum of ferrous FixLN−NO. (b) High-frequency resonance Raman spectra of (A) ferrous FixL*−NO and (B) ferrous FixLN−NO under the same conditions described in part a. (c) High-frequency resonance Raman spectrum of ferrous FixLN−NO at 20 °C with 413.1 nm laser excitation showing (A) perpendicular (⊥) and (B) parallel (∥) polarizations. The difference spectrum (C) is for 5[perpendicular minus 0.157 (parallel)] or 5(⊥ − 0.157∥). The subtraction factor of 0.157 is the depolarization ratio for ν_4 (see part b). The peaks in the difference spectrum correspond to those modes that are more depolarized than ν_4. This difference spectrum clarifies assignment of the depolarized bands ν_{10}, ν_{11}, and ν_{19} as shown. Sample conditions are as described for part a.

high-frequency spectrum obtained for deoxyFixL* is similar to that of deoxyFixLN with its ν_4 at 1355 cm^{-1}. These data indicate that in the absence of ligands the ferrous state of FixLN and FixL* adopts a 5-c high-spin configuration.

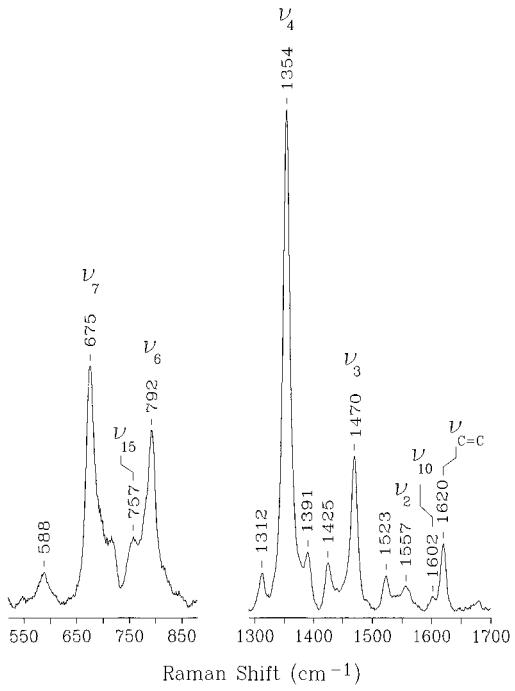

FIGURE 2: Ambient-temperature resonance Raman spectrum of deoxyFixLN with 406.7 nm laser excitation; power = 50 mW. The protein concentration was 70 μM in 80 mM sodium phosphate buffer (pH 7.8) and 5% glycerol.

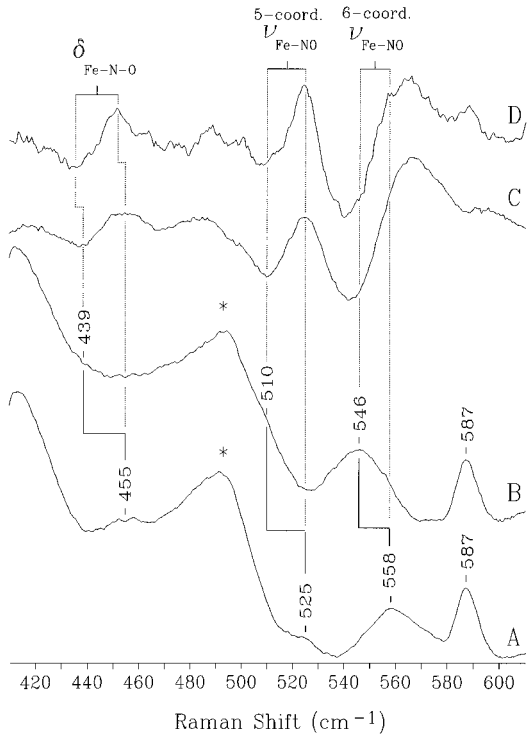

FIGURE 3: Low-frequency resonance Raman spectra of the isotopomeric NO adducts at 20 °C with 406.7 nm excitation: (A) FixLN−^{14}N^{16}O, (B) FixLN−^{15}N^{18}O, (C) 5(FixLN−^{14}N^{16}O minus FixLN−^{15}N^{18}O) difference spectrum, and (D) 5(FixL*−^{14}N^{16}O minus FixL*−^{15}N^{18}O) difference spectrum. The asterisk indicates an underlying glass band.

Figure 3 shows the isotopically sensitive bands in the low-frequency region of the FixLN−NO spectrum at room temperature. The difference spectra generated by subtraction of the spectrum of the ^{15}N^{18}O adduct from that of the respective ^{14}N^{16}O adduct of FixLN and FixL* are included to show that FixL*−NO has the same isotopically sensitive modes as FixLN−NO. This region of the spectrum contains three modes whose frequencies are sensitive to isotopic substitution. The 558 cm^{-1} mode shifts to 546 cm^{-1} in the spectrum of FixLN−^{15}N^{18}O. The isotopic shift and the intensity of this band are consistent with assignment of this mode to the Fe−NO stretching motion for a 6-c FixLN−NO complex [ν(Fe−NO)$_{6-c}$]. It is also similar to the Fe−NO stretching frequencies observed for other 6-c heme−NO adducts as illustrated by the compilation in Table 1. The second band affected by isotopic substitution is revealed most clearly in the difference spectra in Figure 3. This band shifts from 525 to 510 cm^{-1} in the spectra of the FixLN−^{15}N^{18}O and FixL*−^{15}N^{18}O isotopomers. Since this observed frequency and isotopic shift are consistent with those observed for 5-c nitrosyl heme complexes (Deinum et al., 1996; Choi et al., 1991), the 525 cm^{-1} band is assigned to the Fe−NO stretching frequency of 5-c FixLN−NO and FixL*−NO adducts [ν(Fe−NO)$_{5-c}$] (see Table 1). These data indicate that the 6-c and 5-c forms of FixLN−NO and FixL*−NO coexist at room temperature.

Figure 3 reveals a third isotopically sensitive band at 453 cm^{-1} for FixLN−^{14}N^{16}O. This band shifts to 440 cm^{-1} in the ^{15}N^{18}O isotopomer. On the basis of this shift and the frequency of the band in the natural abundance spectrum (Hu & Kincaid, 1991b), the 453 cm^{-1} band is assigned to the Fe−N−O bending mode [δ(Fe−NO)] for the 6-c FixLN−NO. The bending vibration for the 5-c nitrosyl hemes is not observed for FixLN−NO or FixL*−NO. Although the δ(Fe−NO) mode has been reported for other 6-c nitrosyl heme protein complexes (Hu & Kincaid, 1991b) (see Table 1), it has not been observed in the 5-c soluble guanylate cyclase nitric oxide adduct (Deinum et al., 1996) or in model complexes (Choi et al., 1991; Lipscomb et al., 1993). Figure 3 and Table 1 show that the bending mode is shifted to a lower frequency by 3 cm^{-1} in the spectra of FixL*−NO. The isotopic shift of ν(Fe−NO)$_{6-c}$ measured from the original spectra (see Figure 3) is consistent with that determined from the difference spectrum by the method of Laane (1981). The shifts indicated for ν(Fe−NO)$_{5-c}$ and δ(Fe−NO) are based on the maxima and minima of the difference spectra. This was done because of the uncertainty in determining the width and intensities of the original bands.

The 406.7 nm-excited resonance Raman spectra of FixLN−NO and FixL*−NO acquired at 20 and −45 °C are compared in Figure 4. Although the relative enhancement factors for the 5-c and 6-c nitrosyl heme complexes of FixLs are not known, the large difference in the Raman intensities at 558 and 525 cm^{-1} suggests that the 6-c form dominates at room temperature. This is consistent with the relative intensities of the heme core size marker bands for the 5-c and 6-c nitrosyl hemes shown in Figures 1b and 5, which show the dominance of the 6-c bands at room temperature. The ν(Fe−NO)$_{6-c}$ mode is observed at 558 cm^{-1} for both FixLN−NO and FixL*−NO. Although the presence of the kinase domain of FixL does not significantly perturb the frequency of ν(Fe−NO)$_{6-c}$, the band width of this mode is affected. The band widths for ν(Fe−NO)$_{6-c}$ of FixL*−NO and FixLN−NO are 21 and 26 cm^{-1}, respectively. These band widths were obtained by a least-squares fit of the data to a 50% Gaussian, 50% Lorentzian line shape. This combination line shape was shown empirically to accurately model our spectrometer function.

Table 1: Resonance Raman Frequencies and Mode Assignments for Ferrous FixL Nitrosyl Adducts and Other Ferrous Heme Nitrosyl Adducts

adduct	CN[a]	ν(Fe−NO)[b]	δ(Fe−NO)[b]	ν(N−O)	ν_3	ν_8	ν_{10}	temp (°C)	ref[f]
FixLN−NO	5	525 (510)[g]	no	1676	1509	351	1646	20	this work
FixLN−NO	5	526 (513)	no	1664, 1676	1509	349	1646	−45	this work
FixL*−NO	5	525 (510)[h]	no	1675	1509	351	1646	20	this work
FixL*−NO	5	529	no	1675	1509	353	1646	−45	this work
sGC−NO	5	525 (509)	no	1677 (1607)[b]	1509	344	1646	10−20	1
αHbA−NO + IHP	5	nr	nr	1668	1508	nr	1645	nr	2 and 3
Mb−NO + SDS at pH 9.2	5	no	no	no	1512	345	1646	RT[e]	4
FixLN−NO	6	558 (547[c], 546)	453 (440)	no	1498	338	1632	20	this work
FixL*−NO	6	558 (544)	450 (437)	no	1498	338	1632	20	this work
Mb−NO	6	554 (542)	449 (443)	1624 (1587)[d]	1502	342	1638	RT,[e] 0	5−7
HbA−NO	6	555 (533)	450 (443)	1622 (1592)[d]	1500	346	1634	RT,[e] 0	5−7
cytochrome $P450_{cam}$−NO	6	554 (538)	446 (437)	1591 (1537)[b]	1499	352	nr	0	7

[a] CN, coordination number; no, not observed; nr, not reported. [b] Frequencies observed for the $^{15}N^{18}O$ isotopomers in parentheses. [c] ν(Fe−$^{15}N^{16}O$). [d] Frequencies observed for the $^{15}N^{16}O$ isotopomers. [e] Reported at room temperature. [f] The numbers correspond to the following references: (1) Deinum et al. (1996), and (2) Nagai et al. (1980), and (3) Maxwell and Caughey (1976), (4) Mackin et al. (1983), and (5) Tsubaki and Yu (1983), (6) Benko and Yu (1983), and (7) Hu and Kincaid (1991). [g] Full width at half-maximum = 26 cm^{-1}, determined by least-squares fit of the peak by a combination Gaussian−Lorentzian (1:1) line shape. [h] Full width at half-maximum = 21 cm^{-1}, determined by least-squares fit as described above.

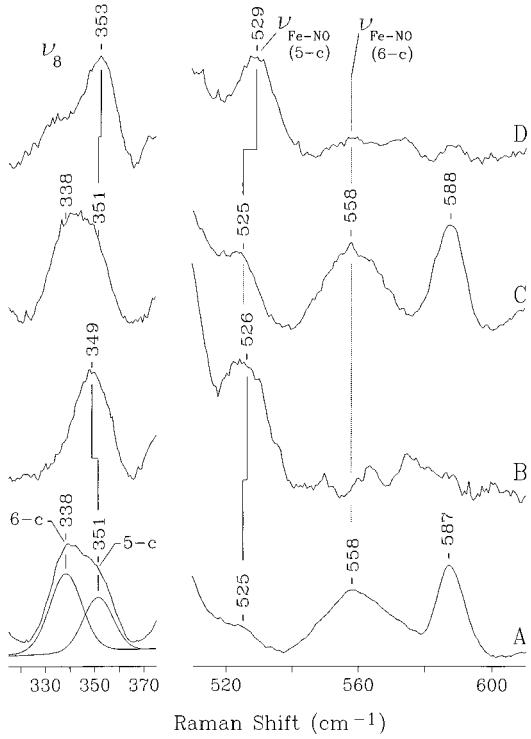

FIGURE 4: Low-frequency resonance Raman spectra (excitation at 406.7 nm) for (A) ferrous FixLN−NO at 20 °C, (B) ferrous FixLN−NO at −45 °C, (C) ferrous FixL*−NO at 20 °C, and (D) ferrous FixL*−NO at −45 °C.

As the temperature of FixLN−NO or FixL*−NO is lowered, the equilibria between the 5-c and 6-c forms of FixLN−NO and FixL*−NO shift toward the 5-c nitrosyl adducts. Spectroscopic evidence for this temperature effect is shown in Figure 4. At low temperatures, bands are observed at 526 and 529 cm^{-1} for FixLN−NO and FixL*−NO, respectively. They are assigned to $\nu(Fe-NO)_{5-c}$ because they exhibit isotope sensitivities similar to those of the 525 cm^{-1} $\nu(Fe-NO)_{5-c}$ bands observed at 20 °C (Table 1). As the temperature is lowered, the $\nu(Fe-NO)_{5-c}$ band becomes more intense at the expense of the $\nu(Fe-NO)_{6-c}$ band, indicating that the 5-c nitrosyl adduct is the predominant species at this temperature. Conversion to the 5-c nitrosyl adduct as the temperature is lowered is further shown by the narrowing of the ν_8 envelope. An accurate fit of the room-temperature ν_8 envelope requires two peaks. The results of this fit are shown in Figure 4a. The ν_8 band at 338 cm^{-1} is more intense than the ν_8 at 351 cm^{-1} at room temperature, and it is diminished in intensity significantly at −45 °C. Therefore, it is assigned to the 6-c nitrosyl adduct which predominates at room temperature. The 351 cm^{-1} band is assigned to $\nu_{8(5-c)}$ for both FixLN−NO and FixL*−NO at room temperature. Upon freezing, small shifts in $\nu_{8(5-c)}$ and $\nu(Fe-NO)_{5-c}$ are observed for both proteins. The band widths for the low-temperature $\nu(Fe-NO)_{5-c}$ bands are 12 and 14 cm^{-1} for FixL*−NO and FixLN−NO, respectively.

The high-frequency region of the resonance Raman spectra of FixLN−NO and FixL*−NO also supports the existence of both 5-c and 6-c nitrosyl adducts for these proteins. Figure 5 shows the high-frequency spectra of FixLN−NO at 20 and −45 °C. In these spectra, the ν_3 frequency serves as an indicator of the coordination number of the nitrosyl FixL adducts (Spiro & Li, 1988). The ν_3 band for FixLN−NO at room temperature (1498 cm^{-1}) is indicative of a 6-c heme. However, this band has a shoulder at 1509 cm^{-1} which corresponds to the 5-c FixLN−NO. As the temperature is lowered, the intensity of the ν_3 band shifts to 1509 cm^{-1}. Shifts to higher frequencies are also observed for other bands in the 1490−1650 cm^{-1} region of the spectrum. The ν_{10} band shifts from 1632 to 1645 cm^{-1}; similar shifts have been observed between 6-c and 5-c nitrosyl adducts of myoglobin and hemoglobin (Table 1). For both ferrous FixLN−NO and FixL*−NO, the conversion from 6-c to 5-c upon lowering of the temperature is completely reversible as shown by the reappearance of $\nu(Fe-NO)_{6-c}$ and ν_3 at their original frequencies, and by the visible spectrum at room temperature.

On the basis of ν(N−O) for other 6-c nitrosyl hemoprotein adducts, the $\nu(N-O)_{6-c}$ bands for FixLN−NO and FixL*−NO are expected to be near 1625 cm^{-1} (Tsubaki & Yu, 1983). Both $\nu(^{14}N-^{16}O)_{6-c}$ and $\nu(^{15}N-^{18}O)_{6-c}$ lie under the more intense bands corresponding to porphyrin ring modes (Figure 5). Because these small bands fall in a crowded region of the spectrum, the $\nu(N-O)_{6-c}$ band could not be assigned for either FixLN−NO or FixL*−NO. The details of this complication are discussed below.

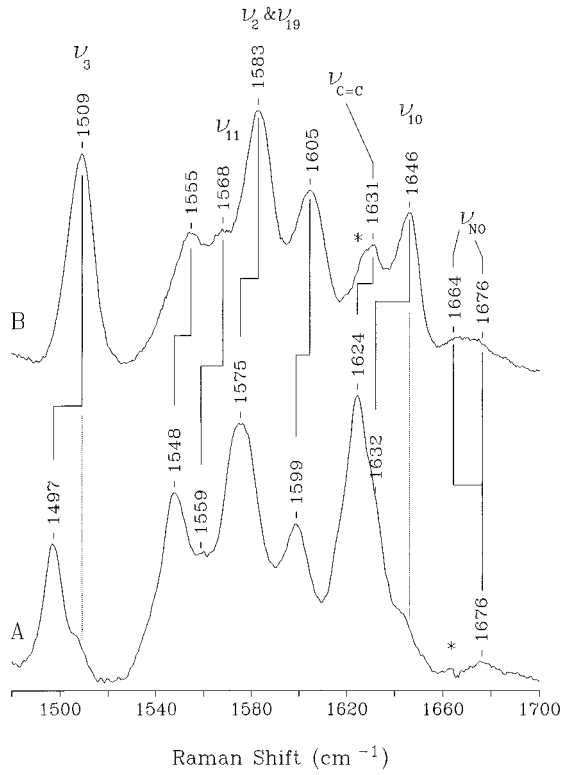

FIGURE 5: High-frequency resonance Raman spectra for ferrous FixLN−NO at (A) 20 °C with 413.1 nm excitation and (B) −45 °C with 406.7 nm excitation. Assignments of in-plane heme vibrations are as in Figure 1c. Solid lines indicate shifts of porphyrin modes to higher frequency and splitting of the NO stretching mode upon formation of the five-coordinate nitrosyl heme at low temperatures. Dotted lines indicate the presence of ν_3 and ν_{10} for the five-coordinate FixLN−NO at room temperature. Asterisks mark the positions of laser plasma lines.

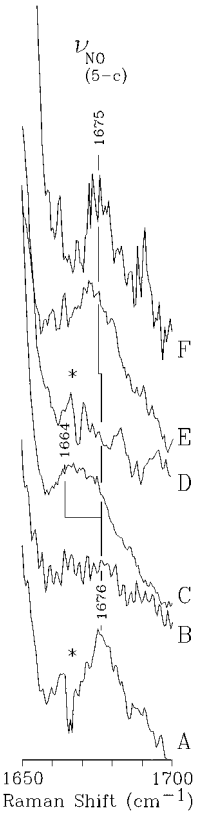

FIGURE 6: ν(N−O) region of the high-frequency resonance Raman spectra of (A) ferrous FixLN−^{14}N^{16}O at 20 °C with 413.1 nm excitation, (B) ferrous FixLN−^{15}N^{18}O at 20 °C with 413.1 nm excitation, (C) ferrous FixLN−^{14}N^{16}O at −45 °C with 406.7 nm excitation, (D) ferrous FixLN−^{15}N^{18}O at −45 °C with 406.7 nm excitation, (E) ferrous FixL*−^{14}N^{16}O at 20 °C with 413.1 nm excitation, and (F) ferrous FixL*−^{14}N^{16}O at −45 °C with 406.7 nm excitation. Sample conditions are as described in Figure 1a. Asterisks mark the positions of laser plasma lines, which were subtracted from A and D.

The resonance Raman spectrum of FixLN−^{14}N^{16}O obtained at 20 °C contains a band at 1676 cm^{-1} (see Figure 6A). In the spectrum of FixLN−^{15}N^{18}O, the 1676 cm^{-1} band is not observed (Figure 6B). If the N−O stretching is modeled by a harmonic oscillator, an isotopic shift of 75 cm^{-1} is predicted for ν(N−O) upon substitution of ^{15}N^{18}O for ^{14}N^{16}O. This would put the ν(N−O) band for FixLN−^{15}N^{18}O at approximately 1600 cm^{-1}, which lies in the crowded region of the spectrum shown in Figure 5. On the basis of its proximity to ν(N−O) for the five-coordinate nitrosyl heme adduct of sGC (Deinum et al., 1996) and its absence at 1676 cm^{-1} in the spectrum of the FixLN−^{15}N^{18}O and FixL*−^{15}N^{18}O adducts, this band is assigned to ν(N−O) for the five-coordinate FixLN−NO [$\nu(N-O)_{5-c}$].

The assignment of $\nu(N-O)_{5-c}$ for FixLN−NO is also corroborated by the resonance Raman data obtained for FixLN−NO at −45 °C. On the basis of ν(Fe−NO) and ν_3 frequencies in Figures 4 and 5, respectively, at −45 °C, the majority of the nitrosyl adducts are in their 5-c form. A broad band centered around 1670 cm^{-1} and containing two components is readily observed in the FixLN−^{14}N^{16}O spectrum (Figure 6C) and is absent from the FixLN−^{15}N^{18}O spectrum (Figure 6D) because it is shifted to a lower frequency. Hence, this envelope is also assigned to $\nu(N-O)_{5-c}$. An accurate fit of this broad envelope requires two peaks, suggesting that at low temperatures there are at least two conformations of the NO ligand in the 5-c FixLN−NO. The 1676 cm^{-1} band corresponds to the FixLN−NO conformation that dominates at room temperature. The high-frequency component of the −45 °C N−O stretching envelope (Figure 6C) occurs at 1664 cm^{-1}, and may arise from population of a second Fe−N−O conformation upon freezing of the FixLN−NO solution. Resonance enhancement of the N−O stretching mode is greater at 413.1 nm than at 406.7 nm. At room temperature, the $\nu(N-O)_{5-c}$ bands are best observed with 413.1 nm excitation because of the greater enhancement. Nevertheless, at low temperatures where the 5-c form of the heme dominates, $\nu(N-O)_{5-c}$ can be observed even with 406.7 nm excitation.

The presence of the kinase domain does not dramatically affect the $\nu(N-O)_{5-c}$ frequency at room temperature (Figure 6E). However, it does stabilize this room-temperature FixL*−NO conformation toward the effects of freezing. In the −45 °C FixL*−NO spectrum, only the one band at 1675 cm^{-1} is observed (Figure 6F) in contrast to the two $\nu(N-O)_{5-c}$ bands observed for FixLN−NO.

DISCUSSION

Thermal Accessibility of the 5-c FixL−NO Adducts. Nitric oxide is well-known as a trans-labilizing ligand in its heme complexes (Scheidt & Piciulo, 1976; Scheidt & Frisse, 1975). In a number of ferrous heme proteins, this effect is sufficient to rupture the proximal iron−ligand bond, yielding 5-c low-spin ferrous nitrosyl heme complexes (Deinum et al., 1996; Winkler et al., 1996; Nagai et al., 1980; Maxwell & Caughey,

1976; Mackin et al., 1983). The labilizing effect of the nitrosyl ligand is also evident in NO adducts of the FixL derivatives examined here. However, the nitrosyl FixLs are unique among the nitrosyl heme proteins because both 5-c and 6-c forms of the nitrosyl heme are present. In αHbA and sGC, Fe−His bond scission is complete so that only the 5-c forms of the NO adducts are observed in the resonance Raman spectra (Deinum et al., 1996; Yu et al., 1994; Nagai et al., 1980). The low- and high-frequency regions of the resonance Raman spectra of the ferrous FixLN−NO and FixL*−NO reveal this 5-c ⇌ 6-c equilibrium in a number of ways. First, at room temperature, ν(Fe−NO) bands for both 5-c and 6-c complexes are observed. Second, the temperature dependence of the resonance Raman spectra of the FixLN and FixL* nitrosyl adducts indicates changes in the ratio of the 6-c to 5-c nitrosyl hemes with decreasing temperatures. Figure 4 shows that at low temperatures $\nu(\text{Fe}-\text{NO})_{5-c}$ becomes significantly more intense than the corresponding $\nu(\text{Fe}-\text{NO})_{6-c}$, indicating that the 5-c form is favored. The temperature dependence of the 6-c:5-c ratio is also evident from variations in the relative intensities of $\nu_{3(6-c)}$ and $\nu_{3(5-c)}$ which track the temperature-dependent shift in the equilibrium between the 6-c and 5-c nitrosyl complexes (K. R. Rodgers, unpublished results). Additionally, Figure 5 shows shifts of ν_2, ν_{10}, ν_{11}, and ν_{19} to higher frequencies, indicative of 5-c heme nitrosyl adducts, as the temperature is lowered. The shifts in these core size marker bands do not arise from ferric FixLN−NO or ferric FixL*−NO, as neither $\nu(\text{Fe}^{\text{III}}-\text{NO})$ nor $\delta(\text{Fe}^{\text{III}}-\text{NO})$ is observed in the low-frequency spectra. For ferric FixLN−NO, we have observed $\nu(\text{Fe}^{\text{III}}-\text{NO})$ and $\delta(\text{Fe}^{\text{III}}-\text{NO})$ at 600 and 575 cm^{-1}, respectively (data not shown), and neither of these bands is observed in the low-frequency spectra in Figure 4. Third, the nitrosyl adducts of both FixL proteins can be reversibly cycled between predominantly 6-c and 5-c forms by appropriate cycling of the temperature. Finally, the presence of the 5-c FixLN−NO and FixL*−NO complexes is shown by ν(N−O) vibrations observed at frequencies characteristic of 5-c nitrosyl heme proteins (Deinum et al., 1996; Maxwell & Caughey, 1976) and model complexes (Choi et al., 1991).

Why Are the Five-Coordinate Nitrosyl Heme Adducts Thermally Accessible in FixL? While the physiological relevance of the accessibility of these two coordination states at ambient temperature is not obvious at this juncture, we offer two possibilities. First, it may be that, because of the denitrification activity exhibited by *R. meliloti* (Chan & Weatcroft, 1993), NO, a denitrification intermediate, is a physiologically relevant ligand for FixL. Since NO-initiated signaling proceeds by scission of the proximal Fe−His bond in soluble guanylate cyclase (Yu et al., 1994; Stone & Marletta, 1994; Stone et al., 1995; Deinum et al., 1996), it is reasonable to contemplate the possibility that Fe−His bond scission in a significant fraction of FixL−NO molecules provides the basis for an sGC-like NO signaling mechanism. The 6-c form of FixL−NO is expected to inactivate the kinase domain via the same spin state change mechanism utilized in O_2 sensing (Gilles-Gonzales et al., 1995), especially since the geometry of the NO adducts appears to mimic the typically bent Fe−O−O moiety. However, the fraction of the protein in its 5-c nitrosyl form could signal the presence of NO via an alternate mechanism analogous to that for sGC, in which the proximal Fe−His bond is cleaved (Stone & Marletta, 1994; Yu et al., 1994; Stone et al., 1995; Deinum et al., 1996). Hence, the NO coordination chemistry of FixL raises the intriguing possibility that it initiates signals in response to NO by two different, and perhaps even parallel, mechanisms. The response initiated would depend upon whether the spin state change mechanism or the proximal bond scission mechanism were activated.

The second possibility centers around the cell's requirement for rapid response to changes in ligand (*i.e.* O_2 or NO) availability. It has been reported that FixL is only about 85% oxygenated in air with 15% remaining in the deoxy state and retaining its kinase activity (Gilles-Gonzalez & Gonzalez, 1993). Hence, it would appear that the cell has a mechanism for maintaining a low level of kinase activity even under atmospheric conditions. Although it is clear that kinase activity is required for transcriptional activation, the lack of significant transcription in air with 15% of FixL exhibiting kinase activity suggests that transcriptional activity is not a necessary consequence of FixL's kinase activity. At high oxygen pressures, the residual 15% of the FixL that remains in the deoxy form continues to undergo autophosphorylation with subsequent phosphotransfer to the response regulator, FixJ. It has been shown that, even if the deoxyFixL−phosphate becomes oxygenated, transfer of the phosphoryl group to FixJ proceeds unabated (Lois et al., 1993). However, it has also been shown that oxyFixL, especially in its phosphorylated form, serves to catalyze the hydrolysis of FixJ−phosphate (Lois et al., 1993). If most of the FixL is in its oxygenated form, the catalytic hydrolysis of FixJ−phosphate must hold the steady state concentration of the transcriptionally activated FixJ−phosphate below the threshold required for effective *nifA* and *FixK* transcription, since significant transcription is not observed under conditions of high oxygen tension. Nevertheless, these counteractive phosphorylation and dephosphorylation reactions may serve to maintain steady state concentrations of FixL− and FixJ−phosphate so that, upon lowering of intracellular O_2 pressure, FixL and FixJ are already present in their phosphorylated forms, thereby minimizing the induction period for buildup of a sufficient FixJ−phosphate concentration for facilitation of *nifA* and *fixK* transcription. In short, the low oxygen affinity of FixLs (Gilles-Gonzalez et al., 1994) may serve to maintain a non-zero steady state concentration of phosphorylated FixL and FixJ in order to facilitate prompt *nifA* and *fixK* transcription in response to decreased oxygen pressure. In this model, changes in intracellular oxygen pressure actually regulate the relative rates of FixJ activation and deactivation by modulating the steady state concentrations of phosphorylated FixL and FixJ.

This model is further supported by the accessibility of 5-c FixL−NO at near-physiological temperature. Since the affinity of the heme for NO is very high in dioxygen-binding heme proteins (Hb affinity for NO is $>10^3$ times its affinity for CO) (Antonini & Brunori, 1971), the presence of even low concentrations of NO is likely to complex most of the protein. If the small percentage of 5-c ferrous FixL*−NO retains its kinase activity, it could be that the small population of 5-c FixL−NO (∼15%; K. R. Rodgers, submitted) serves to maintain its baseline kinase activity, and thus, non-zero steady state concentrations of phosphorylated FixL and FixJ, even at saturating NO levels. Since Fe−His bond scission in the low-spin 5-c NO adduct precludes translocation of the iron into the heme plane from "pulling" on the proximal

His residue as is likely required for loss of kinase activity, it is expected that 5-c FixL−NO will be active. Since the protein solution must be frozen to generate a significant fraction of the protein in its 5-c state, the activity of the 5-c NO adducts cannot be assayed.

Geometry of the Fe−N−O Unit. Both the 5-c and 6-c ferrous FixL−NO adducts exhibit ν(Fe−NO) frequencies very close to those of their Mb and Hb counterparts. Insofar as these frequencies reflect the Fe−NO bond energies, it would appear that the heme environment of FixL does not significantly perturb the stability of the Fe−NO bond relative to those in the other oxygen-binding heme proteins. This is consistent with similarities between the stabilities of the metFixL−CN and met FixL−F and their Mb analogs (Rodgers et al., 1996; Winkler et al., 1996).

The δ(Fe−NO) frequencies observed for both FixLN−NO and FixL*−NO are similar to those observed for ferrous nitrosyl adducts of myoglobin (Mb−NO) and hemoglobin (Hb−NO) (Hu & Kincaid, 1991). The similarities in the frequencies between both ν(Fe−NO) and δ(Fe−NO) for 6-c FixL−NO derivatives and for hemoglobin and myoglobin are consistent with a bent Fe−N−O unit in FixL−NO having an angle near 150° (Deatherage & Moffat, 1979; Hu & Kincaid, 1991).

Assignment of $\nu(N-O)_{5-c}$ is based on its frequency being similar to the corresponding mode in the 5-c sGC−NO adduct and on its absence in the spectrum of the $^{15}N^{18}O$ isotopomer. The $\nu(N-O)_{6-c}$ bands were observed in neither the FixLN−NO nor the FixL*−NO spectra. These bands typically show low resonance enhancements relative to ν_3, ν_{10}, and ν_2, which are sensitive to the ratio of 6- to 5-c nitrosyl FixLs. Since even small variations in temperature elicit measurable change in the 6-c to 5-c population ratio (K. R. Rodgers, unpublished results), the shifts of ν_2, ν_3, ν_{10}, ν_{11}, and ν_{19} illustrated in Figure 5 produce large features in the difference spectra of the NO isotopomers in the region of the spectrum where $\nu(^{14}N-^{16}O)_{6-c}$, $\nu(^{15}N-^{18}O)_{6-c}$, and $\nu(^{15}N-^{18}O)_{5-c}$ are expected (Tsubaki & Yu, 1982; Benko & Yu, 1983; Hu & Kincaid, 1991; Deinum et al., 1996). Hence, observation of the $\nu(N-O)_{5-c}$ and $\nu(N-O)_{6-c}$ difference signals is obstructed for both FixLN−NO and FixL*−NO adducts. In addition to the ν(Fe−NO)-based evidence for a bent Fe−NO unit, the frequency of the $\nu(N-O)_{5-c}$ bands is also consistent with a bent Fe−N−O moiety, as linear M−NO adducts exhibit characteristically higher ν(N−O) frequencies (Hu & Kincaid, 1991a).

Effect of the Kinase Domain on the Distal Heme Pocket and the Fe−N−O Unit. Comparison of the low-frequency resonance Raman spectra for the 6-c nitrosyl complexes of FixLN and FixL* reveals that the regions of the spectra containing the respective ν(Fe−NO) bands are comparable. Although the presence of the kinase domain has been shown to perturb the heme environment for FixL* relative to FixLN (Rodgers et al., 1996), the frequency of $\nu(Fe-NO)_{6-c}$ for these two proteins is insensitive to the perturbation. This is consistent with the observation that ν(Fe−NO) for 6-c Fe^{II}−NO model compounds is rather insensitive to the electron-donating and stereochemical properties of the trans base (Lipscomb et al., 1993). This insensitivity to the properties of the proximal base has also been noted for the ν(Fe−NO) of Fe^{II}−NO adducts of heme proteins. Only small shifts in ν(Fe−NO) are observed in ferrous heme NO adducts when a proximal histidine ligand is replaced by a cysteine ligand (Hu & Kincaid, 1991b) (see Table 1).

The band width of $\nu(Fe-NO)_{6-c}$ in FixL*−NO is 5 cm^{-1} less than that of FixLN−NO. Similar differences in $\nu(Fe-O_2)$ band widths for oxymyoglobin (20 cm^{-1}) and oxycytochrome *c* oxidase (12.9 cm^{-1}) have been reported and attributed to a more tightly fixed ligand geometry at the binding site in cytochrome *c* oxidase (Hirota et al., 1994). Hence, the ν(Fe−NO) band width difference between FixLN−NO and FixL*−NO suggests that the presence of the kinase domain in FixL*−NO supports a more specific interaction between the Fe−N−O unit and the distal heme pocket. We recently suggested that the heme pocket might be shape-selective for bent diatomic ligands (Rodgers et al., 1996). The current evidence for multiple Fe−N−O geometries suggests that shape selectivity is not an important factor in ligand binding since shape selection would also be expected to preclude disorder in the ligand geometry. Recent kinetic evidence further suggests that the heme pocket is less sterically constrained than we had suggested, because large ligands such as imidazole bind rapidly if they are sufficiently basic (Winkler et al., 1996). However, differences in interactions of bound ligands with the heme pockets of FixLN and FixL* are evident. Differences in the steric and/or electrostatic properties of the distal heme pockets of FixL* and FixLN have been suggested on the basis of differences in the ν_4 frequencies of their respective ferrous CO adducts (Rodgers et al., 1996) and by differences in the thermodynamics and kinetics of ligand binding (Rodgers et al., 1996; Winkler et al., 1996; Gilles-Gonzalez et al., 1994).

Differences are also noted in the spectra of the 5-c ferrous nitrosyl complexes of FixLN and FixL*. There is a 3 cm^{-1} increase in the $\nu(Fe-NO)_{5-c}$ frequency for ferrous FixL*−NO relative to that of FixLN−NO at −45 °C. The differences in $\nu(Fe-NO)_{5-c}$ band widths observed for FixLN−NO and FixL*−NO are quite small with $\nu(Fe-NO)_{5-c}$ for FixL*−NO being 2 cm^{-1} narrower than the corresponding band for FixLN−NO. These small spectral differences could arise from differences in the effects of freezing on the structures of the two proteins. Hence, we do not feel that the subtle differences in the spectra of our frozen solutions support structural conclusions.

The observation of one $\nu(N-O)_{5-c}$ frequency in the low-temperature spectrum of FixL*−NO indicates that the presence of the kinase domain stabilizes the room-temperature 5-c FixL*−NO conformation, while others are accessible in FixLN−NO. This further suggests a more specific interaction between the bound NO ligand and the distal heme pocket of FixL*.

Figure 3 reveals that the frequency separation between ν(Fe−NO) and δ(Fe−NO) is 3 cm^{-1} greater for FixL*−NO than for FixLN−NO. Normal-coordinate calculations have shown that the decrease of the Fe−N−O angle results in increased frequency separation of these two modes (Hu & Kincaid, 1991a). Hence, this small difference is consistent with a decreased Fe−N−O angle in FixL*−NO relative to that in FixLN−NO.

Finally, the room-temperature spectra in Figures 1a,b, 3, and 4 reveal that the bands corresponding to the 5-c hemes are more intense in the FixL*−NO spectra than their FixLN−NO counterparts. Specifically, the ν_3, ν_8, ν_{10}, and ν(Fe−NO) bands from the 5-c complexes are more intense in the FixL*−NO spectra. This may reflect increased

proximal tension due to interdomain contacts between the heme and kinase domains of FixL*. However, it is also possible that the increase in the fraction of 5-c nitrosyl heme is an electronic effect associated with the diminished Fe−N−O angle (Hu & Kincaid, 1991b) caused by the aforementioned interaction between the heme and kinase domains.

Implications for Communication between the Heme and Kinase Domains. Hemoglobin is the most well-understood protein from the standpoint of communication of heme ligation and spin state to remote regions of its structure. The subunits of hemoglobin have been shown to have at least two pathways or coordinates for propagation of ligand-initiated conformational motion. These coordinates link the distal and proximal heme pockets to the subunit interface (Perutz, 1979, 1990; Friedman & Lyons, 1980; Friedman et al., 1982; Kaminaka et al., 1990; Ackers et al., 1992; Rodgers et al., 1992; Rodgers & Spiro, 1994; Jayaraman et al., 1995).

The spectroscopic data presented here and that presented previously along with kinetic and thermodynamic evidence (Rodgers et al., 1996; Winkler et al., 1996; Gilles-Gonzalez et al., 1994) are consistent with perturbation of the heme pocket via interplay between the heme and kinase domains of FixL*. This influence of the kinase on the heme verifies the existence of one or more links between the domain interface and the heme pocket. In order for the heme pocket conformation to be influenced by the interaction(s) between the heme and kinase domains, such links must constitute a coordinate along which local conformational change can be propagated between the heme pocket and the points of interdomain contact. Since the kinase domain affects relatively low-energy distortions of the NO ligand geometry, it stands to reason that the larger free energy of NO binding is able to affect conformational changes in the kinase domain along the same link(s). It is thus suggested that propagation of the heme pocket conformational adjustments to NO (or O_2) binding across the domain interface is responsible for remote conformational adjustments in the kinase domain that modulate its reactivity with ATP.

The larger fraction of 5-c nitrosyl heme in FixL*−NO relative to that in FixLN−NO (parts a and b of Figure 1) may also arise in response to a proximal link between the heme pocket and the domain interface in FixL*. This small increase in the population of the 5-c state of the nitrosyl heme corresponds to a slight decrease in the energy separating the 6-c and 5-c states. In other words, the 5-c state is more thermally accessible in FixL*−NO than in FixLN−NO. If this effect is indeed due to a proximal conformational link to the domain interface (as opposed to an indirect electronic effect of the distal Fe−N−O angle), the change in energy separation of these states may be attributable to proximal tension that is associated with the kinase domain and which weakens the Fe−His bond.

Previously, we reported that any influence of the kinase domain on the proximal tension must be small, as we did not observe a measurable shift of ν(Fe−His) between the Soret-excited resonance Raman spectra of deoxyFixLN and deoxyFixL*. Raman spectra acquired in our laboratory with 457.9 nm excitation (unpublished results) also support this conclusion. Other workers have observed the same lack of sensitivity of ν(Fe−His) toward the presence of the kinase on the basis of Raman spectra acquired with 441.6 nm excitation (Kamura et al., 1996). This is borne out by the minimal increase in the thermal accessibility of 5-c FixL*−NO, which corresponds to only about 0.1 kcal, assuming a Boltzmann distribution of states. It is possible that the ν-(Fe−His) frequencies of deoxyFixLN and deoxyFixL* do differ but that the difference is small enough that it cannot be observed due to overlapping of the ν(Fe−His) bands with those of out-of-plane porphyrin vibrations known to occur in this region of the spectrum (Li et al., 1990; Smulevich et al., 1996). Hence, thermal accessibility of the 5-c state serves as a very sensitive indicator of low-energy perturbations in the local structure surrounding the heme in FixL.

SUMMARY

This work reveals the coexistence of 5- and 6-c FixLN−NO and FixL*−NO. The results support a model wherein a low level of FixL kinase activity is maintained, even in the presence of high ligand concentrations. This activity is proposed to serve the role of maintaining a non-zero steady state concentration of FixL and FixJ in their phosphorylated forms to minimize the induction period for transcriptional activation as the ligand (NO or O_2) is depleted. Increased homogeneity in the FixL* Fe−NO conformation over that of FixLN indicates that the kinase domain stabilizes the heme pocket structure, resulting in a preferred heme ligand geometry. This geometry likely serves to direct the free energy of ligand binding into conformational perturbation along the necessary path to affect adjustments in the kinase domain that modulate its reactivity with ATP.

REFERENCES

Abe, M., Kitagawa, T., & Kyogoku, Y. (1978) *J. Chem. Phys. 69*, 4526−4534.

Ackers, G. K., Doyle, M. L., Myers, D., & Daugherty, M. A. (1992) *Science 255*, 54.

Antonini, E., & Brunori, M. (1971) *Frontier in Biology; Hemoglobin and Myoglobin in Their Reacitons with Ligands*, Vol. 21, Chapter 10, North-Holland Publishing Co., Amsterdam.

Benko, B., & Yu, N. T. (1983) *Proc. Natl. Acad. Sci. U.S.A. 80*, 7042−7046.

Chan, Y.-K., & Weatcroft, R. J. (1993) *J. Bacteriol. 175*, 19−26.

Choi, I., Liu, Y., Feng, D., Paeng, K., & Ryan, M. D. (1991) *Inorg. Chem. 30*, 1832−1839.

Choi, S., Spiro, T. G., Langry, K. C., Smith, K. M., Budd, D. L., & LaMar, G. N. (1982) *J. Am. Chem. Soc. 104*, 4345−4351.

Collman, J. P., Gagne, R. R., Reed, C. A., Robinson, W. T., & Ridley, G. A. (1974) *Proc. Natl. Acad. Sci. U.S.A. 71*, 1326−1329.

David, M., Daveran, M. L., Batut, J., Dedieu, A., Domergue, O., Ghai, J., Hertig, C., Boistard, P., & Kahn, D. (1988) *Cell 54*, 671−683.

Deatherage, J. F., & Moffat, K. (1979) *J. Mol. Biol. 134*, 401−417.

Deinum, G., Stone, J. R., Babcock, G. T., & Marletta, M. A. (1996) *Biochemistry 35*, 1540−1547.

Friedman, J. M., & Lyons, K. B. (1980) *Nature 284*, 570.

Friedman, J. M., Rousseau, D. L., Ondrias, M. R., & Stepnoski, R. A. (1982) *Science 218*, 1244.

Galinier, A., Garnerone, A., Reyrat, J., Kahn, D., Batut, J., & Boistard, P. (1994) *J. Biol. Chem. 269*, 23784−23789.

Gilles-Gonzalez, M. A., Ditta, G. S., & Helinski, D. R. (1991) *Nature 350*, 170−172.

Gilles-Gonzalez, M. A., Gonzalez, G., Perutz, M. F., Kiger, L., Marden, M. C., & Poyrart, C. (1994) *Biochemistry 33*, 8067−8073.

Gilles-Gonzalez, M. A., Gonzalez, G., & Perutz, M. F. (1995) *Biochemistry 34*, 232−236.

Hirota, S., Ogura, T., Appelman, E. H., Shinzawa-Itoh, K., Yoshikawa, S., & Kitagawa, T. (1994) *J. Am. Chem. Soc. 116*, 10564−10570.
Hu, S., & Kincaid, J. R. (1991a) *J. Am. Chem. Soc. 113*, 2843−2850.
Hu, S., & Kincaid, J. R. (1991b) *J. Am. Chem. Soc. 113*, 9760−9766.
Jameson, G. B., Rodley, G. A., Robinson, W. T., Gagne, R. R., Reed, C. A., & Collman, J. P. (1978) *Inorg. Chem. 17*, 850−857.
Jameson, G. B., Molinaro, F. S., Ibers, J. A., Collman, J. P., Brauman, J. I., Rose, E., & Suslick, K. S. (1980) *J. Am. Chem. Soc. 102*, 3224−3237.
Jayaraman, V., Rodgers, K. R., Mukerji, I., & Spiro, T. G. (1995) *Science 269*, 1843−1848.
Kaminaka, S., Ogura, T., & Kitagawa, T. (1990) *J. Am. Chem. Soc. 112*, 23.
Kamura, K., Nakamura, H., Tanaka, Y., Oue, S., Tsukamoto, K., Nomura, M., Tsuchiya, T., Adachi, S., Takahashi, S., Iizuka, T., & Shiro, Y. (1996) *J. Am. Chem. Soc. 118*, 9434−9435.
Kitagawa, T., Abe, M., & Ogoshi, H. (1978) *J. Chem. Phys. 69*, 4516−4525.
Laane, J. (1981) *J. Chem. Phys. 75*, 2539−2545.
Li, X.-Y., Czernuszewicz, R. S., Kincaid, J. R., Stein, P., & Spiro, T. G. (1990) *J. Phys. Chem. 94*, 47−61.
Lipscomb, L. A., Lee, B.-S., & Yu, N.-T. (1993) *Inorg. Chem. 32*, 281−286.
Lois, A. F., Weinstein, M., Ditta, G. S., & Helinski, D. R. (1993) *J. Biol. Chem. 268*, 4370−4375.
Mackin, H. C., Benko, B., Yu, N.-T., & Gersonde, K. (1983) *FEBS Lett. 158*, 199−202.
Maxwell, J. C., & Caughey, W. S. (1976) *Biochemistry 15*, 388−396.
Monson, E. K., Weinstein, M., Ditta, G. S., & Helinski, D. R. (1992) *Proc. Natl. Acad. Sci. U.S.A. 89*, 4280−4284.
Nagai, K., Welborn, C., Dolphin, D., & Kitagawa, T. (1980) *Biochemistry 19*, 4755−4761.
Parthasarathi, N., Hanson, C., Yamaguchi, S., & Spiro, T. G. (1987) *J. Am. Chem. Soc. 109*, 3865−3871.
Perutz, M. F. (1979) *Annu. Rev. Physiol. 52*, 1−25.
Perutz, M. F. (1990) *Annu. Rev. Biochem. 48*, 327−386.
Philips, S. E. V. (1980) *J. Mol. Biol. 142*, 531−554.
Piciulo, P. L., Rupprecht, G., & Schiedt, W. R. (1974) *J. Am. Chem. Soc. 96*, 5293−5295.
Reyrat, J., David, M., Blonski, C., Boistard, P., & Batut, J. (1993) *J. Bacteriol. 175*, 6867−6872.
Rodgers, K. R., & Spiro, T. G. (1994) *Science 265*, 1697−1699.
Rodgers, K. R., Su, C., Subramaniam, S., & Spiro, T. G. (1992) *J. Am. Chem. Soc. 114*, 3697−3709.
Rodgers, K. R., Lukat-Rodgers, G. S., & Barron, J. A. (1996) *Biochemistry 35*, 9539−9548.
Rousseau, D. L., & Friedman, J. M. (1988) in *Biological Applications of Raman Spectroscopy* (Spiro, T. G., Ed.) Vol. 3, pp 133−216, John Wiley & Sons, Inc., New York.
Scheidt, W. R., & Frisse, M. E. (1975) *J. Am. Chem. Soc. 97*, 17−21.
Scheidt, W. R., & Piciulo, P. L. (1976) *J. Am. Chem. Soc. 98*, 1913−1919.
Scheidt, W. R., Brinegar, A. C., Ferro, E. B., & Kirner, J. F. (1977) *J. Am. Chem. Soc. 99*, 7315−7322.
Shaanan, B. (1982) *Nature 296*, 683−684.
Smulevich, G., Hu, S., Rodgers, K. R., Goodin, D. B., Smith, K. M., & Spiro, T. G. (1996) *Biospectroscopy 2*, 365−376.
Spaulding, L. D., Cheng, C. C., Yu, N. T., & Felton, R. H. (1975) *J. Am. Chem. Soc. 97*, 2517−2525.
Spiro, T. G., & Li, X. Y. (1988) in *Biological Applications of Raman Spectroscopy* (Spiro, T. G., Ed.) Vol. 3, pp 1−38, John Wiley & Sons, Inc., New York.
Stone, J. R., & Marletta, M. A. (1994) *Biochemistry 33*, 5636−5640.
Stone, J. R., Sands, R. H., Dunham, W. R., & Marletta, M. A. (1995) *Biochem. Biophys. Res. Commun. 207*, 572−577.
Tsubaki, M., & Yu, N. (1982) *Biochemistry 21*, 1140−1144.
Winkler, W. C., Gonzalez, G., Wittenberg, J. B., Hille, R., Dakappagai, N., Jacob, A., Gonzalez, L. A., & Gilles-Gonzalez, M. A. (1996) *Chem. Biol. 3*, 841−850.
Yu, A. E., Hu, S., Spiro, T. G., & Burstyn, J. N. (1994) *J. Am. Chem. Soc. 116*, 4117−4118.

BI9628230